

Thermodynamic Behavior of Poly(cyclohexylethylene) in Polyolefin Diblock Copolymers

Eric W. Cochran and Frank S. Bates*

Department of Chemical Engineering and Materials Science, University of Minnesota, Minneapolis, Minnesota 55455-0132

Received February 11, 2002

ABSTRACT: We report the temperature dependence of the Flory–Huggins interaction parameter for three symmetric diblock copolymer systems containing poly(cyclohexylethylene) (PCHE): poly(cyclohexylethylene-*b*-ethylene) (CE), poly(cyclohexylethylene-*b*-ethylethylene) (CE_E), and poly(cyclohexylethylene-*b*-ethylenepropylene) (CP). Order–disorder transition temperatures (T_{ODT}) were determined using dynamic mechanical spectroscopy and interpreted with mean-field theory, $(\chi/N)_{\text{ODT}} = 10.5$, leading to well-defined expressions for $\chi(T)$. These results have been analyzed in the context of solubility parameter (δ) theory resulting in a unique parameter δ_C that describes the interactions in CE, CP, and CE_E, where $\delta_C < \delta_{\text{EE}} < \delta_P < \delta_E$ with $(\delta_E - \delta_C) \approx 1.6 \text{ MPa}^{1/2}$ at 500 K. In contrast to the predictions of group contribution theory, this indicates that δ_C is in surprisingly close proximity to the solubility parameter for poly(dimethylsiloxane).

Introduction

Polyolefins constitute the most successful class of commercially viable commodities in the polymer industries. The most common examples are the many varieties of poly(ethylene) (PE) and poly(propylene) (PP), which account for the majority of consumer plastics. This success is rooted in remarkably low production costs, a host of useful physical properties, and ease of product fabrication. Physically, polyolefins with highly branched chain architectures exist as low- T_g rubbers while those with more stereoregularity are semicrystalline thermoplastics at use temperatures. Chemically, a polyolefin is simply a fully saturated polymeric hydrocarbon. Lacking reactive chemical moieties, this class of materials is not particularly susceptible to deleterious reactions with oxygen, ozone, acids, or ultraviolet radiation known to plague polydienes and polyaromatics. Furthermore, semicrystalline polyolefins such as PE or isotactic PP are immiscible with essentially all solvents.

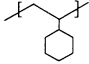
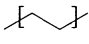
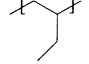
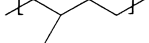
Polyolefins also are attractive materials for studying basic polymer blend thermodynamics. Since the only difference among polyolefins is molecular architecture, simple van der Waals forces dominate the enthalpic contributions to the mixing free energy. One implication for block copolymers is that these weak interactions allow preparation of ordered melts in the weak to intermediate segregation regime at relatively high molecular weight, where non-mean-field fluctuation effects become less important and the chain conformation distribution approaches the Gaussian limit. Another aspect of these simple interactions is that binary polyolefin blends should conform most closely to regular solution models, in contrast to mixtures driven by more polar constituents. A large body of work by Graessley et al.^{1–8} has attempted to treat polyolefin blend thermodynamics with the solubility parameter description. This approach has been moderately successful, with the phase behavior of roughly 75% of the polyolefins studied being well described by a self-consistent set of solubility parameters.

Currently we are interested in polyolefin block copolymers from both fundamental and application-oriented perspectives. Traditionally, the polyolefin family has found limited applications as high-performance engineering plastics due to opacity, inadequate modulus, and other shortcomings. Discovery of catalysts capable of complete, nondegrading saturation of poly(styrene) (PS) has created a new type of commercially viable polymer, poly(cyclohexylethylene) (PCHE). This hydrogenation reaction converts PS into a high modulus ($\sim 1 \text{ GPa}$ at room temperature), higher glass transition temperature material ($T_g \sim 145^\circ\text{C}$ for PCHE compared to 100°C for PS). Unfortunately, because of a large entanglement molecular weight ($\sim 4 \times 10^4 \text{ Da}$),⁹ PCHE is too brittle to be useful as a neat material. This problem can be remedied by incorporation of PCHE into block copolymers along with other rubbery or semicrystalline constituents, ideally other polyolefins such as polyethylene (PE), poly(ethylethylene) (PEE), or poly(ethylenepropylene) (PEP). These four compounds offer a full complement of physical properties, and block copolymers that exploit these attributes can be economically prepared by fully saturating anionically polymerized block copolymers of styrene, butadiene, and isoprene. Table 1 shows the microstructures of these model polyolefins along with their pertinent physical characteristics. We note that the statistical segment length is with respect to a constant reference volume of 118 \AA^3 , approximately corresponding to that of a four-carbon repeat unit at 413 K (e.g., PE or PEE).⁹ β^2 is an established conformational parameter, defined by the relationship¹⁰

$$\beta^2 = \frac{b^2}{6v} \quad (1)$$

where b and v are the statistical segment length and volume, which captures the random walk dimension and coil volume in a single quantity. This index is useful for discussion of segment packing effects in polymer blending, a local phenomenon that is independent of molecular weight.

Table 1. Polymer Physical Property Data at 140 °C

Polymer (Block Notation)	Chemical Structure	M_o , Da	$\frac{M}{N}$, Da ^a	ρ , $\frac{g}{cm^3}$ ^b	b , Å ^c	β^2 , Å ^{-1d}
PCHE (C)		110	65.4	0.92	4.60	0.030
PE ^e (E)		28	55.8	0.78	8.35	0.098
PEE ^e (E _E)		56	57.4	0.81	5.39	0.041
PEP (P)		70	56.2	0.79	6.84	0.066

^a Molar mass with respect to a 118 Å³ monomer reference volume. ^b Mass density. ^c Statistical segment length with respect to reference volume. ^d Conformational parameter comparing radius of gyration to volume, i.e., $\beta^2 = b^2/6v$. ^e PE and PEE contain 2 and 40.9 ethyl branches per 100 backbone carbons.

Block copolymers offer much more complex phase behavior than the analogous homopolymer blends. However, within mean-field treatments both are governed by the same binary segment–segment interaction parameter, the Flory–Huggins parameter χ , which may depend on temperature, pressure, and composition. In this report we restrict our attention to a single composition and pressure and focus on determining $\chi(T)$ for CE, CE_E, and CP. (Table 1 explains the block notation used throughout this article.) These relationships will be exploited in subsequent research directed at the design and evaluation of higher-order polyolefin multiblock copolymers such as CE_EE, CEE_E, and CEE_EEC.

Extraction of $\chi(T)$ from a set of block copolymers is predicated on statistical mechanical theory. Two theoretical treatments, mean-field theory and the fluctuation-corrected version, can be applied in the disordered state or at the order–disorder transition (ODT). Maurer et al.¹¹ have shown that the closest approximation to the $\chi(T)$ expression derived from homopolymer blends is realized when the mean-field result (here for a symmetric composition) (χN)_{ODT} = 10.5 is combined with T_{ODT} measurements. Prior investigations have established $\chi(T)$ for EE_E, EP, and PE_E using this approach.^{11–16} This work adds PCHE to this body of data. We have prepared three sets of symmetric diblock copolymers (CE, CE_E, and CP), totaling 25 compounds, in each case with T_{ODT} located within the experimentally accessible temperature window. T_{ODT} 's were determined using the established dynamic mechanical spectroscopy (DMS) technique and converted to χ values based on mean-field theory. These results are compared with the other polyolefin expressions to which a self-consistent set of solubility parameters can be assigned.

Experimental Section

Precursor Synthesis. The saturated materials used in this study were all prepared by sequential anionic polymerization of styrene, butadiene, and/or isoprene to yield unsaturated block copolymer precursors, which was followed by complete heterogeneous catalytic hydrogenation to yield the desired saturated diblock copolymer. Poly(styrene) (PS) is the precursor to PCHE, 1,4-poly(butadiene) (PB₁₄) is the precursor to PE, 1,2-poly(butadiene) (PB₁₂) is for PEE, and *cis*-1,4-poly(isoprene) (PI) is for PEP.

All monomers and solvents were purified rigorously prior to polymerization according to techniques described elsewhere.¹⁷ For the PS–PI and PS–PB₁₄ diblock precursors, polymerization occurred at 40 °C in cyclohexane under positive argon pressure, using *sec*-butyllithium as the initiator. The active initiator concentration was determined using the Gilman double-titration technique.¹⁸ The reaction sequence began

with the addition of styrene monomer to the initiator/solvent mixture. Formation of the polystyryl anion was indicated by the orange color of the reaction medium. After 8 h, a small aliquot (< 0.1% of the mixture) was cannulated from the reactor and terminated with degassed methanol for molecular weight distribution analysis using size exclusion chromatography (SEC). The reaction continued with the addition of the second monomer, isoprene or butadiene, and was allowed to react for an additional 8 h before termination with degassed methanol. Under these conditions, isoprene is known to favor 95% 1,4-addition and butadiene 93% 1,4-addition.¹⁹

The PS–PB₁₂ diblock precursors were synthesized at 10 °C in cyclohexane and a 100:1 molar ratio of tetrahydrofuran (THF), with respect to the active chains, as a polar modifier. Such conditions accelerate the polymerization of both the poly(styrene) and poly(butadiene) blocks²⁰ and cause the poly(butadiene) block to favor 90% 1,2-addition.¹⁹ Each monomer was allowed to react for at least 4 h to reach 99% completion.

Recovery of all unsaturated precursors was achieved through precipitation at room temperature into a 3:1 mixture of methanol and 2-propanol, followed by drying under dynamic vacuum to constant mass.

Heterogeneous Catalytic Saturation. Saturated polymers were obtained by hydrogenation of the precursor materials. These reactions were conducted in an agitated stainless steel pressure vessel described elsewhere.²¹ A typical saturation reaction consisted of dissolving 5 g of precursor into 500 mL of cyclohexane followed by intense mixing with 0.5 g of a 5% Pt/SiO₂ catalyst^{21–24} for 12 h at 170 °C under 500 psi of H₂. The product materials were recovered by precipitation into a 6:1 mixture of methanol and 2-propanol and dried to constant mass under dynamic vacuum.

Molecular Characterization. Compositions of all materials were determined from integrated ¹H NMR spectra collected on the unsaturated precursor polymers dissolved in deuterated chloroform with a 300 MHz Varian instrument operating at room temperature. Mole fractions of PS, PB₁₄, PB₁₂, and PI were converted to volume fraction PCHE, PE, PEE, and PEP using reported densities at 140 °C (see Table 1).⁹ ¹H NMR also was used to establish the level of saturation in the products; these spectra were obtained at room temperature except for the CE specimens, which required heating to 50 °C to completely dissolve in chloroform. Over 99% saturation was achieved in all the materials discussed here.

Molecular weights were calculated for all specimens using M_n of the PS block of the precursor material (from the aliquot taken during synthesis), as measured with PS-calibrated SEC traces and the mass fraction of the PS block as determined by NMR. SEC also was used to compute the polydispersity of all precursor materials with respect to PS standards, which in every case was less than or equal to 1.04, and to confirm that the saturation process did not lead to any broadening of the molecular weight distribution.

Dynamic Mechanical Analysis. Order–disorder phase transitions were identified through dynamic mechanical spectroscopy (DMS) measurements conducted with a Rheometrics

Table 2. Characterization Data for the CE, CE_E, and CP Diblock Copolymers

polymer	M_n , kDa ^a	M_w/M_n	N_n ^b	f_C ^c	T_{ODT} ^d , °C
CE-1	12.8	1.02	192	0.54	168
CE-2	13.2	1.02	198	0.55	172
CE-3	13.6	1.02	205	0.54	180
CE-4	15.6	1.02	240	0.52	227
CE-5	16.2	1.02	247	0.53	234
CE-6	16.4	1.02	257	0.52	250
CE-7	16.9	1.03	256	0.53	263
CE-8	17.0	1.03	260	0.52	266
CE _E -1	29.7	1.03	462	0.50	< $T_{g,C}$
CE _E -2	31.8	1.03	499	0.49	< $T_{g,C}$
CE _E -3	36.2	1.02	563	0.50	< $T_{g,C}$
CE _E -4	37.9	1.02	601	0.48	184
CE _E -5	39.0	1.03	609	0.50	177
CE _E -6	40.6	1.02	631	0.50	180
CE _E -7	46.9	1.03	720	0.51	236
CE _E -8	53.1	1.02	825	0.50	273
CE _E -9	62.3	1.02	973	0.50	335
CP-1	18.1	1.02	278	0.52	139
CP-2	20.1	1.02	312	0.50	175
CP-3	21.4	1.02	330	0.51	190
CP-4	21.4	1.02	318	0.55	192
CP-5	22.0	1.02	352	0.48	208
CP-6	22.0	1.02	341	0.51	201
CP-7	23.4	1.02	359	0.51	243
CP-8	24.6	1.02	378	0.52	253

^a As calculated from mass fraction and M_n of precursor S block.^b Polymerization index with respect to a reference volume $v = 118 \text{ \AA}^3$.^c Volume fraction C, based on densities reported at 140 °C.⁹^d As determined by the discontinuity in the elastic modulus during isochronal temperature ramp.

Scientific ARES strain-controlled rheometer fitted with 25 mm parallel plates. Samples were compression-molded into 25 mm \times 1 mm disks for 5–10 min at 500 psi and 160 °C, which is above $T_{g,C}$, the highest thermal transition in these systems. Samples were heated under nitrogen in the rheometer to roughly 10 °C above T_{ODT} to erase any thermal history and then cooled to 135 °C prior to beginning the isochronal temperature ramp experiment. In all cases the heating rate was 1 °C/min. Strain amplitude initially was set to 1% but was automatically increased to as high as 5% as necessary to maintain a sufficient torque signal. This limit was chosen so that all measurements were taken within the linear viscoelastic regime. A single frequency of 1 rad/s was employed for all measurements. This corresponds to $\omega < \omega_c(T)$ throughout the observed temperature range, where $\omega_c(T)$ represents the crossover frequency separating domain and entanglement dynamics.^{25,26}

Results and Analysis

The characterization data of all samples produced for this study appear in Table 2. PS-calibrated SEC traces allowed the accurate ($\pm 5\%$) determination of M_n for the PS block in each of the precursor materials. This information along with the NMR composition data was used to calculate M_n for each of the saturated diblock copolymers.

On the basis of the near-symmetric compositions, the lamellae morphology is expected for all polymers. Gehlsen et al. report lamellae based on small-angle neutron scattering analysis for individual CE,^{27,28} CE_E,²⁸ and CP^{12–14,16,29} samples that lie within our composition and molecular weight ranges. (Because of a limited number of specimens, Gehlsen and co-workers did not determine $\chi(T)$.) Isothermal frequency scans taken below the T_{ODT} for each specimen showed a nonterminal low-frequency response with $G' \approx G'' \sim \omega^{1/2}$, which is consistent with the lamellae morphology. Several rep-

resentative small-angle X-ray scattering (SAXS) measurements (not shown here) confirmed this assessment.

DMS has been established as a sensitive technique for detecting phase transitions in block copolymer melts.^{25,26} For brevity, one set of representative isochronal temperature sweeps of $G'(T)$, with heating and cooling, is shown for each of the three saturated systems investigated in Figure 1. The storage moduli undergo a slow exponential decay during heating to the point of a sudden discontinuity that we associate with the ODT. Both the heating and cooling transitions occur over a 2 °C temperature window. Hysteresis between heating and cooling transitions was less than 10 °C when the diblock samples were heated and cooled at 1 °C/min. When the heating rate was reduced, the temperature of the order-to-disorder transition remained stationary while the ordering temperature rose toward that of the disordering transition; ordering from the spatially homogeneous state is governed by nucleation,^{30–32} while disordering is essentially a barrier-free process. Thus, reported T_{ODT} values, ranging from 139 °C up through 335 °C (Table 2), were obtained during heating. These transition temperatures span the experimentally accessible range, bounded below by $T_{g,C} \approx 140$ °C. We did not find evidence of thermal degradation during the rheology measurements as evidenced by agreement within experimental error of T_{ODT} with repeated measurements and invariant SEC traces.

Within mean-field theory, and for model symmetric A–B diblock copolymers (volume fraction $f_A = 1/2$, and $b_A = b_B$ where b is the statistical segment length), the ODT occurs at a fixed interaction strength, $(\chi N)_{ODT} = 10.5$. The polymers listed in Table 2 fail to satisfy the symmetric condition. While the volume fractions are all reasonably symmetric, conformational symmetry, i.e., $b_A = b_B$, is violated for all three pairs. Furthermore, the mean-field value does not account for composition fluctuation effects, which suppress the formation of an ordered state to higher values of χN . These effects have been treated theoretically by Fredrickson and Helfand,³³ which are manifested as an additive correction to $(\chi N)_{ODT}$ that vanishes for large values of N .

In principle, ignoring these deviations from symmetry and fluctuation effects in utilizing the mean-field ODT prediction to extract χ introduces a slight systematic error into the values we report; however, this error does not detract from the qualitative features of our results. Furthermore, while convincing experimental evidence indicates that fluctuation effects are important,^{12,16,34} use of fluctuation-corrected interaction parameters with the nonfluctuation corrected mean-field theory is not appropriate. Thus, the interaction parameters appearing in Table 2 were calculated by evaluating the relationship

$$\chi_{AB}(T_{ODT}) = \frac{10.5}{N} \quad (2)$$

where N is normalized to the arbitrary but somewhat conventional reference volume of 71.1 cm³/mol (118 Å³), the molar density of most four-carbon polyolefin segments (e.g., E_E and E) at 140 °C. Figure 2 plots $\chi(T)$ data for the PCHE-containing diblocks measured in this work, which illustrate an excellent correlation with the conventional form $\chi(T) = A/T + B$. Least-squares fits to the data are plotted as solid lines in Figure 2. $\chi(T)$ correlations drawing from published data for E_EP,^{12–14,16,35} E_EE,^{14–16,29} and EP^{11,16} diblocks are also provided for

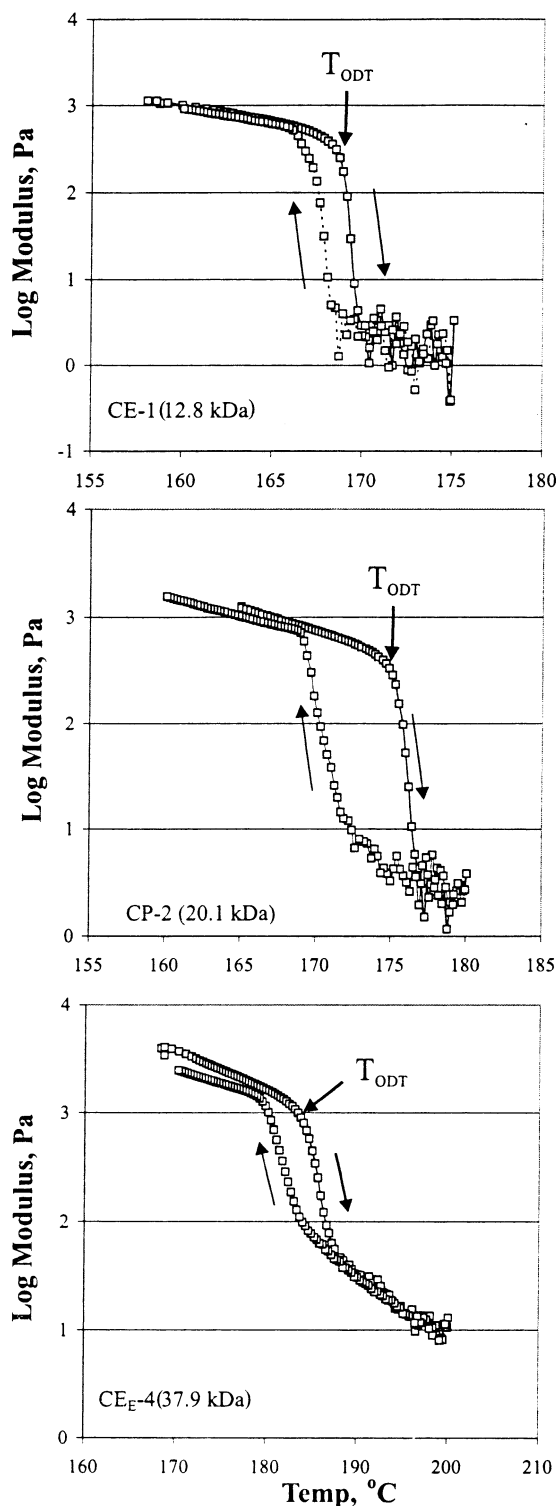


Figure 1. Dynamic elastic modulus (G') during isochronal frequency scans used to determine T_{ODT} for CE, CE_E, and CP diblock copolymers. Heating and cooling rate is 1 °C/min. Arrows show the direction of heating/cooling. Frequency is $\omega = 1$ rad/s, and strain was kept below 5% in every instance.

comparison (dashed lines). The numerical results of these correlations are listed in Table 3.

Discussion

Graessley and co-workers¹⁻⁸ have developed an extensive body of data concerning the thermodynamic interactions in blends of polyolefins. This group found

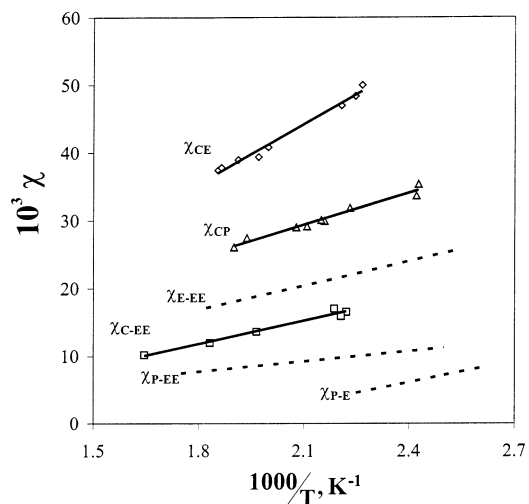


Figure 2. Temperature dependence of $\chi_{AB}(T_{ODT}) = 10.5/N$ for diblock copolymers of C, E, E_E, and P. Data points correspond to the materials characterized in Table 2, and solid lines are correlations thereof. Dashed lines are correlations for χ_{EE} , χ_{EEP} , and χ_{PE} , taken from previously published results.¹¹⁻¹⁶

Table 3. Correlations of the Form $\chi_{AB} = A/T + B$ for the Flory Interaction Parameter in Fully Saturated Polyolefin Diblock Copolymers

binary pair	A, K	$B \times 10^3$	binary pair	A, K	$B \times 10^3$
CE	29.4	-17.4	E _E E ¹⁶	12.0	-4.5
CE _E	11.2	-8.7	E _E P ¹⁶	4.9	-0.5
CP	15.7	-3.6	EP ¹¹	8.9	-16.2

for roughly 75% of the blends studied, termed "regular" mixtures, that the thermodynamics were well described by regular solution theory and the solubility parameter concept. Cast in terms of the Hildebrand equation,³⁶ this yields

$$\chi_{AB} = \frac{v}{kT}(\delta_A - \delta_B)^2 \quad (3)$$

where δ_i is the solubility parameter for component i , v is the reference volume, and k is Boltzmann's constant. Since the interactions in polyolefin mixtures reflect mainly dispersive van der Waals forces, the only type considered by Hildebrand in the development of the theory, saturated hydrocarbons are the most likely polymers to conform to eq 3. Graessley et al. were able to assign a unique magnitude δ_i to each regular homopolymer by extraction of the value $(\delta_A - \delta_B)$ from χ_{AB} measured for each mixture. For the regular mixtures these values were self-consistent, meaning that

$$(\delta_A - \delta_B) = (\delta_A - \delta_C) - (\delta_B - \delta_C) \quad \text{or} \quad \chi_{AB} = (\sqrt{\chi_{AC}} - \sqrt{\chi_{BC}})^2 \quad (4)$$

Irregular polyolefin blends cannot be so correlated and may even produce negative χ parameters, clearly outside the limits of eqs 3 and 4. More sophisticated treatments such as the PRISM³⁷⁻⁴² or lattice cluster theories⁴³⁻⁴⁷ are required to account for these effects.

Almdal et al.⁴⁸ recently have applied this approach to rationalize the binary interactions of PE, PEE, and PEP with poly(ethylene oxide) (PEO) and poly(dimethylsiloxane) (PDMS) using another series of symmetric diblock copolymers. With the exception of the diblock copolymers containing PEO, $\chi_{AB}(T)$ was found to lead to a self-consistent set of δ_i s in every instance. We

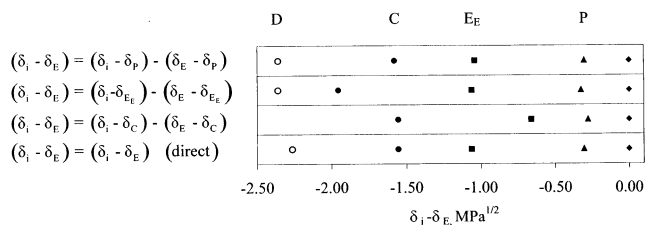


Figure 3. Solubility parameters of C, E, E_E, P, and D at 500 K, referenced to δ_E . The row labeled “direct” plots values calculated from Hildebrand’s equation using interaction parameters as calculated from Table 3 or ref 48 for δ_D . The remaining rows are indirect calculations for δ_i that test for consistency.

analyze our own data in this way to see where PCHE lies in this scheme of solubility parameters. Figure 3 compares the solubility parameters for PDMS, PE, PEE, PEP, and PCHE at 500 K. These were calculated using values of $|(\delta_A - \delta_B)|$ extracted from eq 3. $\chi_{AB}(T)$ is evaluated using the correlations in Table 3 or in the cases of the PDMS-containing specimens those published by Almdal et al.⁴⁸ The absolute ordering of the δ ’s was determined by Graessley et al. in their examinations of deuterium label swapping effects on blend interactions.^{1,3} The values are referenced to δ_E , the largest of the materials under consideration. The row denoted as “direct” in Figure 3 plots $(\delta_i - \delta_E)$ as calculated directly from χ_{iE} as per eq 3, while the other rows demonstrate the self-consistency of the parameters by reconstructing $(\delta_i - \delta_E)$ indirectly through eq 4.

We illustrate in Figure 3 that with the possible exception of the PCHE–PEE pair all binary mixtures formed from these five materials show regular behavior. At 500 K, $(\delta_C - \delta_E) = 0.90 \text{ MPa}^{1/2}$ as calculated directly from χ_{CE} , while the indirect calculations predict that $(\delta_C - \delta_E) \sim 0.5 \text{ MPa}^{1/2}$.

Another interesting feature of Figure 3 is the close proximity of δ_C to δ_D , the solubility parameter for PDMS. Intuitively, we expected the interaction strength between PCHE and PDMS to be large; PCHE is comprised mostly of $-(\text{CH}_2)-$ groups like PE, and the density is more than 15% greater than the other model polyolefins. However, on the basis of our solubility parameter analysis, which is plausible since PCHE and PDMS are both accommodated by the self-consistent scheme, we find that $(\delta_C - \delta_D) \sim 0.4 - 0.8 \text{ MPa}^{1/2}$, the smallest of all the PCHE-based polymer pairs investigated. Symmetric diblock copolymers with this degree of compatibility require approximately $M_n = 5 \times 10^4$ Da to place T_{ODT} in the neighborhood of 200 °C. Confirmation of this prediction would provide a useful validation of the solubility parameter approach. That δ_C is smaller than the solubility parameter of all other polyolefins also implies that this component will preferentially wet the air interface in blends and block combinations. Such placement of a high- T_g component at the surface should impact a variety of applications where surface hardness, and a reduced surface tension, are important.

Unknown solubility parameters are often estimated for materials using group contribution methods such as that developed by Van Krevelen.⁴⁹ However, this approach is frequently quite unreliable. For this set of materials the Van Krevelen method fails to recover the qualitative experimental behavior of these materials, with $\delta_{E_E} < \delta_P \ll \delta_C < \delta_E$, where experimentally we find that $\delta_C < \delta_{E_E} < \delta_P < \delta_E$.

Solubility parameters may be measured directly according to the PVT relationship:³⁶

$$\delta_i = \left(T \frac{\alpha(T)}{\beta(T)} \right)^{1/2} \quad (5)$$

where $\alpha(T)$ is the thermal expansion coefficient and $\beta(T)$ is the isothermal compressibility. The considerable amount of experimental uncertainty in PVT solubility parameter measurements is greatly amplified when considering the quantity $|(\delta_A - \delta_B)|$. However, even with this consideration, the agreement of $|(\delta_A - \delta_B)|$ values derived from published polyolefin PVT data^{2,7,8} with those derived from the $\chi(T)$ values reported here is qualitatively poor.⁵⁰ This disagreement may indicate that some characteristic of diblock copolymer thermodynamics is not well-suited to the solubility parameter description. Perhaps one such aspect is the experimentally determined excess entropic contribution to χ , embodied in the B term of $\chi(T)$, which introduces a type of temperature dependence into the quantity $|(\delta_A - \delta_B)|$ not accounted for by the PVT relationship. This contribution is quite strong in the PCHE systems studied in this work. Regardless of their correspondence to true solubility parameters, the values δ_i computed in this work nevertheless exhibit self-consistency much as do the polyolefin blends of Graessley et al.

Previous reports have identified an apparent connection between the magnitude of χ and the disparity in statistical segment length b .^{4,14,28,48,51} This correlation was first noted by Bates et al. for diblock copolymers of PE, PEE, PEP, and a PE/PEE random copolymer.¹⁴ Gehlsen and Bates²⁸ and Graessley et al.⁴ provided further evidence for this correlation based on experiments conducted with diblock copolymers and binary blends, respectively. Several theoretical treatments have addressed this issue, leading to mixed and in some cases conflicting conclusions. Fredrickson and co-workers^{14,51,52} have proposed an excess entropic contribution to χ , χ_e , that is the result of conformational rearrangements that must accompany the random mixing of two coils of different sizes. In polyolefins the χ_e term has the potential to be the dominant contribution to χ , since the enthalpic component is so small with respect to other monomer types. This statistical theory predicts that

$$\chi_e = \frac{\Lambda_b^3 v}{24\pi^2} \left[\frac{1 - (\beta_A^2/\beta_B^2)^2}{f - (1 - f)(\beta_A^2/\beta_B^2)^2} \right]^2 \quad (6)$$

where $\Lambda_b > b$ is a cutoff length that separates the local and nonlocal conformational regimes. However, Graessley et al.⁴ trace the correlation between b and χ back to enthalpic (i.e., solubility parameter) effects and demonstrate a linear trend in δ with respect to b for a large number of blends. Almdal et al.⁴⁸ proffer a different enthalpically based mechanism. Species with larger statistical segment lengths offer more area per volume for polymer–polymer contacts, which is equivalent to having a larger coordination number z in the classical Flory–Huggins formulation of χ :

$$\chi = \frac{z}{kT} \left(\epsilon_{12} - \frac{1}{2}(\epsilon_{11} + \epsilon_{22}) \right) \quad (7)$$

where ϵ_{ij} is the interaction energy between sites of type i and j . Under this so-called “ z -effect”, there should be

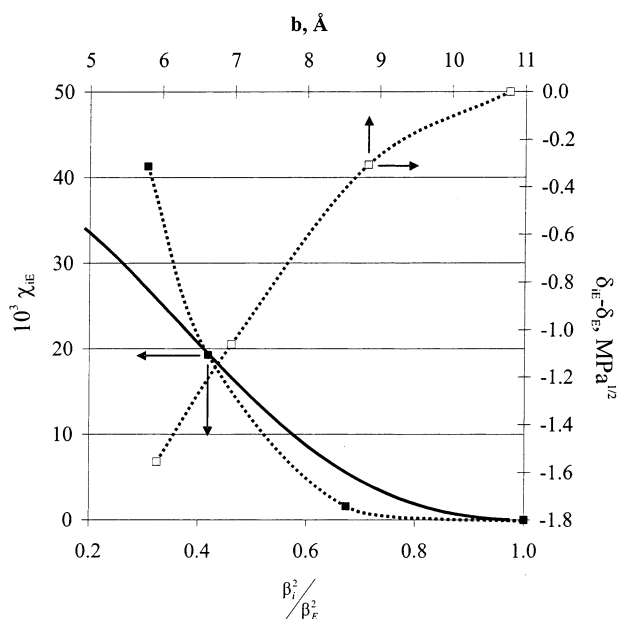


Figure 4. Relationships demonstrating the dependence of interaction strength on conformational asymmetry at 500 K for C, E, E_E, and P. χ_{EE} vs β_i^2/β_E^2 (■) conforms qualitatively to the theory of Fredrickson et al. (see eq 6) with a cutoff length of $\Lambda = 0.93$ Å (—). On the secondary axes $(\delta_i - \delta_E)$ vs b (□) is plotted. The dashed lines are provided as guides to the eye.

stronger interactions between polymers that have more extended coils, i.e., those with larger β^2 parameters (eq 1).

The interaction strength in PCHE-containing polyolefin diblocks also seems to increase with increasing conformational asymmetry. However, the data from this study neither strongly support nor refute any of the various arguments referred to above. In Figure 4, χ_{EE} vs β_i^2/β_E^2 and $(\delta_i - \delta_E)$ vs b for PCHE, PE, PEE, and PEP are plotted at 500 K. The first representation of the data allows for direct comparison with the Fredrickson theory. A reasonable fit of the χ_{EE} data to eq 6 is obtained with $\Lambda_b = 0.93$ Å (plotted as a solid curve in Figure 4), which is an indication that the spirit of the theory is correct. However, the cutoff length required for a good fit is unreasonably low to be interpreted as the boundary between local and nonlocal effects. The second method of interpreting the data follows the Graessley argument that conformational effects are related to the solubility parameter. The δ_i appear to trend roughly linearly with b , as was found earlier by Graessley et al. for blends. These trends are disrupted, however, by the inclusion of species that are not polyolefins. For instance, PDMS, which obeys solubility parameter self-consistency, has conformational characteristics nearly identical to those of E_E with $b = 6.9$ Å and $\beta_D^2 = 0.041$, but $\chi_{DE} > 4\chi_{EE}$. This highlights that the interactions in nonpolyolefinic materials are more complex, and other factors may diminish the importance of conformational asymmetry on the effective interaction parameter. Here we note that the more complete theoretical treatments of Schweizer et al.^{37–42} and Freed et al.^{43–47} have the capacity to account for the nonideal aspects of our results. However, for molecular design purposes, the χ correlations reported in Table 3 are adequate for guiding the synthesis of more complex multiblock copolymers as shown in a separate report.⁵³

Summary

We have investigated the thermodynamic interactions of PCHE with several of the traditional fully saturated polyolefins: PE, PEE, and PEP. Through measurement of the T_{ODT} in symmetric diblock copolymers at various molecular weights we were able to extract the Flory–Huggins segment–segment interaction parameter χ as a function of temperature through the application of the mean-field result $(\chi N)_{ODT} = 10.5$. While these data are only strictly valid for anticipating the thermodynamic behavior of symmetric diblock copolymers, we report in a future publication⁵³ the utility of the mean-field $\chi(T)$ along with the random phase approximation in the design of higher-order block copolymers.

PCHE was found to interact with PE, PEP, and PEE in a way that is well represented by regular solution theory. That is, there exists a unique solubility parameter δ_C that correctly predicts the interaction strengths of the pairs CE, CP, and CE_E. Comparison of δ_C to δ_D ⁴⁸ indicates that if PCHE and PDMS form a regular mixture that the interaction between them should be quite weak, on the same order of magnitude as the PEP–PE interaction.

Finally, the general trend of increasing interaction strength with conformational asymmetry was again noted for the diblocks considered in this study, in support of both entropic and enthalpic arguments. However, this trend is by no means universal for all polymers, particularly those outside of the family of hydrocarbon isomers such as PDMS or that feature polar interactions such as PEO.

Acknowledgment. This work was made possible by the NSF through a fellowship to E.W.C. and Grant NSF/DMR-9905008.

References and Notes

- Graessley, W. W.; Krishnamoorti, R. *Macromolecules* **1993**, *26*, 1137–1143.
- Graessley, W. W.; Krishnamoorti, R.; Balsara, N. P.; Butera, R. J.; Fetters, L. J.; Lohse, D. J.; Schulz, D. N.; Sissano, J. A. *Macromolecules* **1994**, *27*, 3896–3901.
- Graessley, W. W.; Krishnamoorti, R.; Balsara, N. P.; Fetters, L. J.; Lohse, D. J.; Schulz, D. N.; Sissano, J. A. *Macromolecules* **1994**, *27*, 2574–2579.
- Graessley, W. W.; Krishnamoorti, R.; Reichart, G. C.; Balsara, N. P.; Fetters, L. J.; Lohse, D. J. *Macromolecules* **1995**, *28*, 1260–1270.
- Lohse, D. J.; Garner, R. T.; Graessley, W. W.; Krishnamoorti, R. *Rubber Chem. Technol.* **1998**, *72*, 569–578.
- Reichart, G. C.; Graessley, W. W.; Register, R. A.; Lohse, D. J. *Macromolecules* **1998**, *31*, 7886–7894.
- Reichart, G. C. Ph.D. Thesis, Princeton University, Princeton, NJ, 1997.
- Krishnamoorti, R.; Graessley, W. W.; Balsara, N. P.; Lohse, D. J. *Macromolecules* **1994**, *27*, 3073–3081.
- Fetters, L. J.; Lohse, D. J.; Richter, D.; Witten, T. A.; Zirkel, A. *Macromolecules* **1994**, *27*, 4639–4646.
- Vavasour, J. D.; Whitmore, M. D. *Macromolecules* **1992**, *25*, 5477–5486.
- Maurer, W. W.; Bates, F. S.; Lodge, T. P.; Almdal, K.; Mortensen, K.; Fredrickson, G. H. *J. Chem. Phys.* **1998**, *108*, 2989–3000.
- Bates, F. S.; Rosedale, J. H.; Fredrickson, G. H. *J. Chem. Phys.* **1990**, *92*, 6255–6270.
- Bates, F. S. *Macromolecules* **1989**, *22*, 2557–2564.
- Bates, F. S.; Schulz, M. F.; Rosedale, J. H. *Macromolecules* **1992**, *25*, 5547–5550.
- Zhao, J.; Majumdar, B.; Schulz, M. F.; Bates, F. S.; Almdal, K.; Mortensen, K.; Hajduk, D. A.; Gruner, S. M. *Macromolecules* **1996**, *29*, 1204–1215.

- (16) Rosedale, J. H.; Bates, F. S.; Almdal, K.; Mortensen, K.; Wignall, G. D. *Macromolecules* **1995**, *28*, 1429–1443.
- (17) Ndoni, S.; Papadakis, C. M.; Bates, F. S.; Almdal, K. *Rev. Sci. Instrum.* **1995**, *66*, 1090–1095.
- (18) Gilman, H.; Cartledge, F. K. *J. Organomet. Chem.* **1964**, *2*, 447–454.
- (19) Jones, T. Ph.D. Thesis, University of Minnesota, Minneapolis, MN, 2000.
- (20) Schulz, M. F.; Khandpur, A. K.; Bates, F. S.; Almdal, K.; Mortensen, K.; Hajduk, D. A.; Gruner, S. M. *Macromolecules* **1996**, *29*, 2857–2867.
- (21) Gehlsen, M. D. Ph.D. Thesis, University of Minnesota, Minneapolis, MN, 1993.
- (22) World Intellectual Property Organization WO 96/34896.
- (23) U.S. Patent 5,612,422.
- (24) U.S. Patent 6,090,359.
- (25) Rosedale, J. H.; Bates, F. S. *Macromolecules* **1990**, *23*, 2329–2338.
- (26) Gehlsen, M. D.; Almdal, K.; Bates, F. S. *Macromolecules* **1992**, *25*, 939–943.
- (27) Weimann, P. A.; Hajduk, D. A.; Chu, C.; Chaffin, K. A.; Brodil, J. C.; Bates, F. S. *J. Polym. Sci., Part B: Polym. Phys.* **1999**, *37*, 2053–2068.
- (28) Gehlsen, M. D.; Bates, F. S. *Macromolecules* **1994**, *27*, 3611–3618.
- (29) Lipic, P. M.; Bates, F. S.; Matsen, M. W. *J. Polym. Sci., Part B: Polym. Phys.* **1999**, *37*, 2229–2238.
- (30) Kim, W. G.; Chang, M. Y.; Garetz, B. A.; Newstein, M. C.; Balsara, N. P.; Lee, J. H.; Hahn, H.; Patel, S. S. *J. Chem. Phys.* **2001**, *114*, 10196–10211.
- (31) Balsara, N. P.; Garetz, B. A.; Newstein, M. C.; Bauer, B. J.; Prosa, T. J. *Macromolecules* **1998**, *31*, 7668–7675.
- (32) Hashimoto, T.; Sakamoto, N.; Koga, T. *Phys. Rev. E: Stat. Phys., Plasmas, Fluids, Relat. Interdiscip. Top.* **1996**, *54*, 5832–5835.
- (33) Fredrickson, G. H.; Helfand, E. *J. Chem. Phys.* **1987**, *87*, 697–705.
- (34) Glinka, C. J. *Phys. Rev. Lett.* **1988**, *61*, 2229–2232.
- (35) Rosedale, J. H.; Bates, F. S. *J. Am. Chem. Soc.* **1987**, *110*, 3542–3545.
- (36) Hildebrand, J. H.; Scott, R. L. *The Solubility of Non-Electrolytes*, 3rd ed.; Van Nostrand-Reinhold: Princeton, NJ, 1950.
- (37) Singh, C.; Schweizer, K. S. *Macromolecules* **1995**, *28*, 8692–8695.
- (38) Singh, C.; Schweizer, K. S. *Macromolecules* **1997**, *30*, 1490–1508.
- (39) Schweizer, K. S. *Macromolecules* **1993**, *26*, 6050–6067.
- (40) Schweizer, K. S.; Singh, C. *Macromolecules* **1995**, *28*, 2063–2080.
- (41) David, E. F.; Schweizer, K. S. *Macromolecules* **1995**, *28*, 3980–3994.
- (42) Singh, C.; Schweizer, K. S. *J. Chem. Phys.* **1995**, *103*, 5814–5832.
- (43) Dudowicz, J.; Freed, K. F. *J. Chem. Phys.* **1994**, *100*, 4653–4664.
- (44) Freed, K. F.; Dudowicz, J. *Trends Polym. Sci. (Cambridge, U.K.)* **1995**, *3*, 248–255.
- (45) Freed, K. F.; Dudowicz, J. *Macromolecules* **1998**, *31*, 6681–6690.
- (46) Dudowicz, J.; Freed, K. F.; Douglas, J. F. *Phys. Rev. Lett.* **2002**, *88*, 095503/095501–095503/095504.
- (47) Dudowicz, J.; Freed, K. F. *Macromolecules* **1991**, *24*, 5076–5095.
- (48) Almdal, K.; Hillmyer, M. A.; Bates, F. S. *Macromolecules*, submitted for publication.
- (49) Van Krevelen, D. W. In *Properties of Polymers*, 3rd ed.; Elsevier: Amsterdam, 1997; pp 189–226.
- (50) For instance, PVT data indicate that $\chi_{EP} = 0$ at 83 °C. In contrast, extensive experimental studies of this system have shown expressly UCST behavior.
- (51) Liu, A. J.; Fredrickson, G. H. *Macromolecules* **1992**, *25*, 5551–5553.
- (52) Bates, F. S.; Fredrickson, G. H. *Macromolecules* **1994**, *27*, 1065–1067.
- (53) Cochran, E. W.; Bates, F. S. *Macromolecules*, submitted for publication.

MA020227+